

# **Day the Solar Wind Almost Disappeared: Magnetic Field Fluctuations, Wave Refraction and Dissipation**

Charles W. Smith, Dermott J. Mullan, and Norman F. Ness

Bartol Research Institute, University of Delaware, Newark

Ruth M. Skoug and John Steinberg

Los Alamos National Laboratory, Los Alamos, New Mexico

Short title: DAY THE SOLAR WIND DISAPPEARED

**Abstract.** On May 11, 1999 the ACE spacecraft observed a rarefied parcel of solar wind. This has come to be known as *The Day the Solar Wind Disappeared*. Little if any change is seen in the large scale interplanetary magnetic field during this time, but the magnetic field fluctuations are depressed and significantly more transverse to the mean field. The high Alfvén speed resulting from the constant field intensity and low ion density enhances wave refraction and we examine this as a possible explanation for the fluctuation properties. The solar wind possesses a very low proton  $\beta$ , thereby separating the cyclotron and ion inertial length scales and permitting a test of possible dissipation dynamics. We find that the test favors the ion inertial scale theories.

## 1. Introduction

Midday on May 10, 1999 the ACE spacecraft observed the beginning of a period of depleted solar wind ion density that continued until midday on May 12 with a density minimum that lasted  $\sim 6$  hours at the end of May 11. During this extended forty-eight hour period the density dropped from a fairly typical value of  $\sim 5 \text{ cm}^{-3}$  to  $\sim 0.1 \text{ cm}^{-3}$ . We hereafter refer to this entire forty-eight hour period as the “rarefaction interval” without intending to attribute any particular source explanation [*Usmanov et al., 2000*]. During this interval the Alfvén speed was exceptionally high while the ion temperature and wind speeds were low. The exceptional nature of this parcel of solar wind provides an opportunity to examine in some detail two distinct physical processes that operate in the solar wind. One involves macrophysics (refraction) and the other involves microphysics (dissipation).

As regards macrophysics, some of what we do here draws its inspiration from solar physics. MHD waves propagate through the magnetically structured corona in a predictable manner. Specifically, fast-mode waves are refracted away from regions of high Alfvén speed [*Uchida, 1973*]. Conversely, fast-mode waves are focused towards regions of low Alfvén speed. These conclusions are valid in the limit of ray optics, i.e. in cases where the wavelength of the fast-mode MHD wave is short compared to typical scale-sizes of coronal magnetic structures.

*Uchida [1973]* has shown that these results provide a useful context for understanding the propagation of flare-induced disturbances (“Moreton waves”) through the corona.

In confirmation of this, some striking examples of Moreton waves have been detected recently by the EIT instrument on SOHO [*Thompson et al.*, 1999]. In a study of  $\sim 200$  EIT wave events, *Meyers and Thompson* [private communication, 2001; manuscript in preparation] report the waves are indeed consistently refracted away from regions of high Alfvén speed.

The significance of these results in the present context is as follows. The rarefaction interval is a region of exceptionally high Alfvén speed (at times in excess of  $300 \text{ km s}^{-1}$ ). The spatial extent of the parcel of solar wind that engulfed the ACE spacecraft during the rarefaction interval was of order  $10^{12} \text{ cm}$ , much larger than the wavelength of MHD fast-mode waves with periods of a few hours or less. The parcel is therefore large enough to validate the application of ray optics to all but the longest period waves. On the basis of Uchida’s work, we expect that the May 10–12 observation should have the property that fast-mode waves are refracted away from the parcel. That is, the interior of the parcel should, in effect, prohibit propagation of fast-mode waves into it.

As regards microphysics, we note that magnetic dissipation processes may, in principle, be significantly affected within the extraordinary interval of rarefaction. For the last 30-some years, it has seemed that cyclotron damping of parallel-propagating Alfvén waves might be responsible for the dissipation of magnetic fluctuations in the solar wind [*Coleman*, 1968; *Behannon*, 1975]. Evidence in favor of cyclotron damping seems to be provided by the empirical result that the spectral break frequency  $\nu_{\text{bf}}^{\text{obs}}$  between the shallower inertial range and steeper dissipation range of the spectrum happens to be close to the (Doppler-shifted) ion-cyclotron frequency  $\Omega_{ic} = eB/m_{\text{PC}}$  in

many data sets [Schwartz *et al.*, 1981]. However, recent work [Leamon *et al.*, 1998a,b] has demonstrated that the decades-old claim for cyclotron damping is not as strong as was once believed. In fact Leamon *et al.* [1999, 2000] point out that the  $\nu_{\text{bf}}^{\text{obs}}$  data in many parcels of solar wind are more consistent with two alternative and distinct physical mechanisms that operate at the ion inertial scale. The fact that the plasma  $\beta$  in the solar wind at 1 AU is typically of order unity has the effect that the length scale  $L_{ic} = V_{th}/\Omega_{ic}$  (where  $V_{th}$  is the ion thermal speed) associated with ion cyclotron resonance happens to coincide with the ion inertial length  $L_{ii} = V_A/\Omega_{ic}$  where  $V_A$  is the Alfvén speed.

This coincidence does not occur in the interval under study in this paper. The parcel of plasma observed is remarkably rarefied and cold, and as a result, the values of  $L_{ii}$  and  $L_{ic}$  become widely separated. This feature allows us to perform a meaningful comparison of the above competing theories.

We do not attempt to address the source of the rarefied parcel of solar wind of interest to us here. Other authors have made suggestions concerning its origin [Richardson *et al.*, 2000; Usmanov *et al.*, 2000; Crooker *et al.*, 2000]. The present paper addresses aspects of the magnetic fluctuations during the three days in question. We show that the magnetic fluctuations possess an unusual degree of anisotropy that is associated with the period of low plasma density. Moreover, fluctuations in the magnitude of the field are generally smaller than those commonly seen in the solar wind. We discuss the possibility that wave refraction is responsible for the observed depletion of magnetic fluctuation energy within the rarefaction interval. We examine

the dissipation range spectrum and test two current theories for its formation and the resulting dissipation of magnetic energy in the solar wind. We close this paper with a discussion of several possibly related observations made by the Ulysses spacecraft.

## 2. Observations

The analysis discussed here focuses on ACE observations during three days in 1999. Magnetic field measurements are supplied by the MAG instrument [*Smith et al.*, 1999] and thermal particle measurements are provided by the SWEAPAM instrument [*McComas et al.*, 1999]. The defining feature of this period is a prolonged and deep depletion of the solar wind density that begins on DOY 130 and extends until midday on DOY 132. At the same time that the density is low, the solar wind speed and ion temperature are found to be reduced. The following analysis focuses on the magnetic fluctuations during this time.

### 2.1. Overview

Figure 1 shows an overview of the plasma and field measurements during May 10–12, 1999 (DOYs 130–132). The interplanetary magnetic field, IMF, magnitude  $B$ , field latitude  $\delta$  and longitude  $\lambda$  are shown in the top three panels. The most notable feature of these data is their unexceptional nature. The IMF magnitude and direction on DOY 131 are more steady than on the days before and after, but this is not unusual. There is no depletion of the field magnitude.

The fourth panel shows the root-mean-square fluctuation level of the IMF,  $B_{\text{RMS}}$ ,

computed for 16-s intervals. We draw attention to the fact that  $B_{\text{RMS}}$  is unusually small (0.1-0.2 nT) during the rarefaction interval. Before and after this interval,  $B_{\text{RMS}}$  is close to 1 nT. Thus, during the rarefaction interval,  $B_{\text{RMS}}$  undergoes a factor of 5-10 reduction compared to the neighboring plasma. We will examine the physical significance of this large reduction below.

The fifth through seventh panels show the radial component  $V_R$  of the solar wind velocity  $V_{\text{SW}}$ , the proton density  $N_P$ , and proton temperature  $T_P$ . The wind speed is seen to decrease monotonically from midday of DOY 130 until  $\sim 18:00$  UT on DOY 131 followed by a particularly low wind speed during the last 6 hours of DOY 131. At the same time the proton density is decreasing through  $\sim 2$  orders of magnitude with a minimum at  $\sim 18:00$  UT on DOY 131. The proton temperature is unusually low for typical solar wind observations during the last 6 hours of DOY 131, but *Richardson et al.* [2000] demonstrate that  $T_P$  and  $V_{\text{SW}}$  display the nominally expected correlation for solar wind observations.

The eighth panel in Figure 1 shows the computed plasma  $\beta = 8\pi N_P k_B T_P / B^2$  where  $k_B$  is Boltzmann's constant. The most striking feature of this panel is that during the rarefaction interval,  $\beta$  falls to very small values, of order  $10^{-3}$ . This has several implications. First, we can rewrite  $\beta = 2V_{\text{th}}^2 / V_A^2$  where  $V_{\text{th}} = \sqrt{k_B T_P / m_p}$  is the thermal speed of the protons and  $V_A = B / \sqrt{4\pi N_P m_P}$  is the Alfvén speed. Typical solar wind conditions near Earth have  $\beta \simeq 1$ , i.e.  $V_{\text{th}} \simeq V_A$ . However, during the rarefaction interval, when  $\beta$  falls below 0.01,  $V_A$  and  $V_{\text{th}}$  become unequal by at least one order of magnitude.

To see the significance of  $\beta \neq 1$ , we note that  $\beta$  can be expressed as the ratio of the two significant length scales:  $\beta = 2L_{\text{ic}}^2/L_{\text{ii}}^2$ . As *Leamon et al* [2000] point out, the length scales  $L_{\text{ic}}$  and  $L_{\text{ii}}$  play significant roles in two competing theories for the dissipation of magnetic energy and heating of thermal particles in the solar wind. Therefore, the low- $\beta$  event in the rarefaction interval offers a nearly unique opportunity to test and contrast these two theories. We pursue this opportunity in a later subsection.

Panel nine shows the computed Alfvén speed. The low density, in combination with the nearly constant IMF intensity, leads to an elevated Alfvén speed during this time. The simultaneously decreasing wind speed leads to nearly sub-Alfvénic wind flow during the last 6 hours of DOY 131. It should be noted that there is a factor of 2–4 uncertainty on  $N_P$  and  $T_P$  during this time because the energy-dependent instrument response leads to larger measurement uncertainty at these low wind speeds. For this reason values of  $V_A > 350 \text{ km s}^{-1}$  are not plotted. This adds uncertainty to the question of whether sub-Alfvénic flow is, in fact, achieved.

Panels ten and eleven in Figure 1 show the computed anisotropy of the fluctuating components of the magnetic field vectors in two distinct frequency ranges (inertial and dissipation). The anisotropies are computed from the ratio of the magnetic fluctuation energy in the two components perpendicular to the mean field (summed) to the energy in the parallel component of the fluctuation  $(E_x^B + E_y^B)/E_z^B = E_{\perp}^B/E_{\parallel}^B$  where we adopt the mean-field coordinate definitions of *Belcher and Davis* [1971]. The energies  $E_{\perp}^B$  and  $E_{\parallel}^B$  are determined by fitting the power spectra over an appropriate range of frequencies using a power law form, and then comparing the fitted spectra. Horizontal

bars represent the data interval used in the analysis while vertical bars give the variance of the computed ratio. Two frequency ranges are used: panel ten refers to the inertial range and panel eleven refers to the dissipation range analyses. The exact frequency ranges used in each case vary due to considerations that will be presented below when the spectra of specific time intervals are shown. Generally, the inertial range is taken to be  $2 \times 10^{-3}$  to  $(1-2) \times 10^{-1}$  Hz, while the dissipation range is taken to be  $\sim 0.2-0.9$  Hz.

The key feature of the anisotropy panels is that during the period of low solar wind density the IMF fluctuations in the inertial and range are distinctly more transverse to the mean field than elsewhere. *Belcher and Davis* [1971] state that the typical IMF fluctuations in the inertial range possess an anisotropy  $E_{\perp}^B/E_{\parallel}^B$  that is on average 9:1. We find that on May 10-12, 1999, the anisotropy  $E_{\perp}^B/E_{\parallel}^B$  is significantly smaller than average before and after the interval in question, but more than twice the average value during the period of lowest solar wind density. On May 11, 1999 the inertial range fluctuations are exceptionally transverse and demonstrate high anisotropy ( $E_{\perp}^B/E_{\parallel}^B > 20:1$  and exceeding 28:1). Transverse fluctuations are frequently cited as an indication for the presence of Alfvén waves and we will return to this interpretation below. Turning to the dissipation range, we see that the fluctuations are generally less transverse, in keeping with *Leamon et al.* [1998a], and show a less significant rise during the rarefaction interval. However, many questions remain regarding the dissipation processes and it is likely that dissipation may be responsible for the reduced anisotropy in this frequency interval.

Several recent studies have attempted to resolve the orientation of wave vectors

in the interplanetary medium [*Bieber et al.*, 1996; *Leamon et al.*, 1998a]. Both studies have shown that in the inertial range on average only 20% of the fluctuation energy at 1 AU is associated with wave vectors that are parallel to the mean field (1-D or slab geometry generally regarded as parallel-propagating waves). The remaining 80% of the fluctuation energy is associated with wave vectors that are normal to the mean field (2-D turbulence). The analysis technique on which these studies is based assumes a partition between the two options and is not completely general. *Leamon et al.* [1998a] show that typically 46% of the dissipation range spectrum is composed of slab geometry fluctuations. The bottom two panels in Figure 1 use this same analysis technique on intervals within the three days studied here. It must be stated that not all data intervals we have examined yield physically realistic results (slab fractions between 0 and 100%) and this technique continues to be experimental when applied to individual intervals of data (the statistical significance of this method is less in question). However, it is interesting to note that the percent slab geometry in the inertial range early in the rarefaction interval (when  $V_A \leq 50 \text{ km s}^{-1}$ ) is consistently higher than previously seen by *Bieber et al.* and *Leamon et al.* However, when ACE lies deep inside the rarefaction interval, the slab fraction is consistent with the earlier analyses. There appears to be an enhancement of the slab wave component early and late in the three-day period when  $V_A$  is more nearly typical of solar wind values at 1 AU, but a depletion of the slab component deep within the rarefaction interval where  $V_A$  is high. The dissipation range behavior is less clear, but still generally higher than normal. With only one exception at the beginning of the three-day period, the percent slab component is higher in the

dissipation range than in the inertial range. From the apparent fact that our three-day interval is more wavelike than typical IMF observations, we will argue below that (1) wave refraction is (or has been) effective at attenuating the wave component within the region of high Alfvén speed leading to reduced RMS levels there, and yet (2) dissipation processes remain most effective on the 2-D component as argued by *Leamon et al.* [1998a, 1999, 2000].

## 2.2. Reduced IMF Fluctuation Level

We now take a closer look at several of the results concerning magnetic field fluctuations presented above. We start with the observed reduction in  $B_{RMS}$ . Figure 2 shows the distribution of  $B_{RMS}$  levels for ACE/MAG measurements spanning the period DOY 1, 1998 through DOY 169, 2000. As above, each data value used to construct the distribution is the RMS value of the fluctuations about a 16-s mean as computed from  $3 \text{ vs}^{-1}$  measurements. The distribution peaks at  $\sim 0.2 \text{ nT}$ , but exhibits a long tail extending to  $1.5 \text{ nT}$  and beyond. In order to demonstrate the relative rarity of RMS levels  $< 0.2 \text{ nT}$ , we integrate the distribution function in the lower panel. The computed value for  $\int_0^{0.1} Pd(B_{RMS}) = 0.02$  while  $\int_0^{0.2} Pd(B_{RMS}) = 0.24$ ,  $\int_0^{0.5} Pd(B_{RMS}) = 0.74$  and  $\int_0^{1.0} Pd(B_{RMS}) = 0.93$ . This indicates that while  $B_{RMS}$  levels which range from 0.5 to 1.0 both before and after DOY 131 are larger than the median value, the levels during DOY 131 tend to the lower limits of the distribution.

Why are the magnetic fluctuations so small in amplitude during the rarefaction interval? We suggest that refraction effects [*Uchida, 1973*] are at work. The principal

basis for our suggestion is the fact that  $V_A$  is locally enhanced. As Uchida has shown, it is a general result in the limit of ray optics that fast-mode waves are refracted away from regions of high  $V_A$ . The rarefaction interval is a high- $V_A$  region *par excellence* for solar wind observations. Not only does this explain the reduced RMS level within the rarefaction interval, but it also accounts for the enhanced slab fraction outside the rarefaction interval, on both sides of the interval. It appears that the slab waves have been “channelled” into (and possibly accumulated within) the surrounding low- $V_A$  plasma.

If the refraction process is at work in the solar wind in general, we expect that  $B_{\text{RMS}}$  values should anti-correlate with  $V_A$  values. To test this possibility, we start by computing the mean  $B_{\text{RMS}}$  value for magnetic fluctuations as a function of  $V_A$  in the general solar wind. Figure 3 shows the result of this search. We use MAG and SWEFAM observations from DOY 34 of 1998 (when SWEFAM was activated) through DOY 183 of 2000. Intervals of  $30 \text{ km s}^{-1}$  are used in binning  $V_A$ . The top panel shows the distribution when 64-s MAG data averages are used without further analysis (SWEFAM’s resolution is 64 s and the MAG data is averaged to the same timing). Values of  $V_A > 400 \text{ km s}^{-1}$  are not shown due to low confidence in these data. Vertical uncertainties denote the variance of individual binned distributions while horizontal uncertainties denote the width of the  $V_A$  bins. The distribution is relatively flat, with little indication of variation.

What is not considered in the top panel of Figure 3 is that a region of finite size is needed for refraction to be effective. For instance, regions smaller than about one

wavelength in linear extent will not refract waves effectively. We are considering a range of wavelengths in the solar wind, and so we consider a range of possible scale sizes for the refraction regions. The bottom 4 panels of the figure are all constructed by requiring that a data interval of finite duration possess nearly invariant values of  $V_A$  (all 64-s values within the interval must fall in the same  $V_A$  bin). If it does, the corresponding values of  $B_{\text{RMS}}$  are averaged and a single value is entered into the accumulating distribution. The requirement of finite interval length reduces some  $V_A$  bins to sets of zero measure. What can be seen in Figure 3 is that the highest ranges of  $V_A$  do in fact hint at depleted  $B_{\text{RMS}}$  levels once the data intervals reach sufficient size. Moreover, the corresponding minimum  $V_A$  for which depletion is seen becomes smaller with increasing scale size.

Thus, the anti-correlation that is expected from the refraction hypothesis may be present in the general solar wind data.

Of course, the analysis is affected by decreasing statistics. All of the reduced  $B_{\text{RMS}}$  levels associated with higher  $V_A$  are obtained from only a few or a single data interval so that in some instances no calculable uncertainty can be obtained. In other cases, when only a few intervals are available, the uncertainty is genuinely small, smaller than the symbol used in plotting. We believe that the reproducible trend is suggestive, but not conclusive, evidence that wave refraction away from high values of  $V_A$  is occurring in the solar wind. The theory is also consistent with the rarefaction interval that is the primary subject of study in this paper.

### 2.3. Magnetic power spectra: reduction of compressive modes

We have selected five intervals from the three days of data: (a) 130/0:00–12:00 UT, (b) 130/12:00–18:00 UT, (c) 131/6:00–24:00 UT, (d) 132/0:00–12:00 UT, and (e) 132/6:00–24:00 UT and we have computed the power spectral density (PSD) for these five data intervals. Figure 4 shows the trace of the PSD matrix (total power in the fluctuations), the PSD for the component parallel to the mean field, and the PSD of the magnetic field magnitude time series. Intervals (a) and (b) are prior to and early in the onset of the density decrease. Interval (c) includes the region of minimum  $N_P$  while (d) coincides with the rising phase of  $N_P$  near the end of the event. Interval (e) is largely following the recovery of  $N_P$  to normal values.

The first observable result when comparing the trace spectra in the five panels is that all of the power levels are depleted during the rarefaction interval, in keeping with the trend of the 16-s  $B_{\text{RMS}}$  values. To aid in seeing this result, we have performed a power law fit to the inertial range of the trace spectrum in panel (a) and reproduced this fit as a dashed line in all five panels. While the fit curve is not readily evident in panel (a) as it lies beneath the trace spectrum, it is clear that the trace spectrum in panel (c) is reduced by a factor of  $\sim 5$  relative to the power in panels (a), (b), (d) and (e). (The trace spectrum in (b) is actually reduced slightly relative to the trace spectrum in (a) while the trace spectra in (d) and (e) are actually elevated slightly relative to the trace spectrum of (a) and the associated fit line.)

We draw attention to a significant feature in panel (c) (the rarefaction interval).

During this interval, the ratio of the spectrum of the parallel component to the trace spectrum is significantly smaller than in the other intervals. This indicates that there is a significant increase of the transverse component relative to the parallel component during the times of low  $N_P$ . This is particularly evident in panel (c), but the beginning of this trend can also be seen in panel (b). Since the spectra of the parallel fluctuations (labelled Par in the figure) are associated with compressive fluctuations, we conclude that in the interval represented by panel (c), the solar wind is significantly less compressive than in the other intervals. This is consistent with the refraction hypothesis which predicts that in the high- $V_A$  region (panel (c)), there should be exclusion of fast-mode waves (i.e. those with compressions), whereas the Alfvénic modes (i.e. those which are transverse and non-compressive) should not be affected.

Comparison of the trace PSD with the magnetic field magnitude spectra demonstrates that the relative level of the field magnitude fluctuations is reduced during the period of low  $N_P$ . The PSD of the magnitude is always reduced relative to the trace, but this reduction is particularly pronounced in panels (c) and (d).

All three of the observed spectral decreases (the reduced level of the trace spectra, the reduced level of the parallel fluctuation spectra relative to the trace, and the reduced level of the magnitude spectra relative to the trace) during the period of depressed  $N_P$  are seen to recover in the last panel once  $N_P$  has also recovered to normal levels.

## 2.4. Dissipation

Considerable attention has recently been paid to the dissipation of magnetic fluctuations in the solar wind and the associated heating of the thermal particles [Zank *et al.*, 1996; Matthaeus *et al.*, 1999; Smith *et al.*, 2000]. Cyclotron damping of parallel-propagating Alfvén waves [Stix, 1992] has been a favorite explanation for the dissipation of magnetic fluctuations in the solar wind [Coleman, 1968]. However, as an argument against cyclotron resonance, Leamon *et al.* [1998a] conclude that cyclotron resonant damping of parallel-propagating Alfvén waves fails to predict accurately the break frequency in the spectrum of IMF fluctuations. They reach this conclusion by considering how the cyclotron resonance frequency should to vary as a function of changing solar wind conditions (including the winding angle). Leamon *et al.* find that the observations do not support these predictions. In view of this, Leamon *et al.* [1999, 2000] argue that dissipation is *not* controlled by cyclotron resonance, but rather is associated with processes that act at the ion inertial scale. In the present paper, the rarefaction interval, with its exceptionally low  $\beta$ , offers an ideal opportunity to further test the hypothesis of Leamon *et al.*

In order to test the inertial length scale hypothesis, we now turn to a determination of the frequency  $\nu_{\text{bf}}^{\text{obs}}$  where the spectrum makes a transition to the dissipation range. Figure 5 presents, on an expanded scale, the trace spectra shown in Figure 4. The inertial and dissipation ranges can be clearly resolved, along with the break frequency  $\nu_{\text{bf}}^{\text{obs}}$ . The labels (a)–(e) represent the same five panels from Figure 4 and their associated

time intervals. We compute fits of both inertial and dissipation ranges to power laws, and then compute  $\nu_{\text{bf}}^{\text{obs}}$  (including statistical errors) from the intersection of the two power laws. The locations of the spectral break frequencies in each subset is indicated by arrows in Figure 5 and numerical values of  $\nu_{\text{bf}}^{\text{obs}}$  are listed in Table 1.

The significant conclusion from Figure 5 and in Table 1 is that as the spacecraft moves more deeply into the rarefaction interval, the spectral break point shifts toward lower spacecraft frequencies. Then as the spacecraft emerges into the ambient wind,  $\nu_{\text{bf}}^{\text{obs}}$  returns to higher values, somewhat in excess of the original values. The reduction of  $\nu_{\text{bf}}^{\text{obs}}$  in the rarefaction interval is highly significant: in panel (c),  $\nu_{\text{bf}}^{\text{obs}}$  is less than the values in panels (a) and (e) by at least  $10\sigma$ .

To understand how this compares with the theoretical predictions, we first note that in the rarefaction interval the Alfvén speed  $V_A$  increases by a factor of almost 10 while the thermal speed  $V_{\text{th}}$  simultaneously decreases by a factor of about 3. Since  $B$  remains constant, the ion cyclotron scale  $L_{\text{ic}}$  decreases (by about 3) as the spacecraft enters the rarefaction interval whereas the proton inertial scale  $L_{\text{ii}}$  simultaneously increases by about a factor of 10. Doppler shifting of the spatial scales to spacecraft frame frequencies,  $\nu^{\text{obs}}$ , is accomplished by noting that  $k_{\text{ii,ic}} = 2\pi/L_{\text{ii,ic}}$  and  $\nu^{\text{obs}} = (\mathbf{k} \cdot \mathbf{V}_{\text{SW}})/(2\pi) + \omega/(2\pi)$  where  $\omega$  is the wave frequency in the plasma frame. Note that in the rarefaction interval,  $V_{\text{SW}}$  falls by a factor of about 1.3 relative to ambient wind. Neglecting for the moment any question of the orientation of  $\mathbf{k}$  relative to  $\mathbf{V}_{\text{SW}}$ , we can now predict how the two values of  $\nu^{\text{obs}}$  should behave in the rarefaction interval.

First, we consider cyclotron resonance. Since  $\omega$  in this case is essentially  $\Omega_{\text{ic}}$  and

$B$  remains constant, there is no change in this term in the rarefaction interval. The increase in  $k_{ic}$  by a factor of about 3 outweighs the factor 1.3 decrease in  $V_{SW}$ . Therefore, if cyclotron resonance damping is at work, there should be a net increase in  $\nu_{bf}^{obs}$  when the spacecraft enters the rarefaction interval.

Turning now to the ion inertial scale, the ten-fold decrease in  $k_{ii}$  is strengthened by the factor of 1.3 decrease in  $V_{SW}$  to predict a large decrease in the  $(\mathbf{k} \cdot \mathbf{V}_{SW})/(2\pi)$  term in  $\nu_{bf}^{obs}$  if the ion inertial scale marks the onset of dissipation. In the case of inertial-length processes, it is less obvious what frequency should be used for the  $\omega$  term in  $\nu^{obs}$ . If low frequency waves are involved, then  $\omega$  is probably a fraction of the value of  $\Omega_{ic}$ . Since  $\Omega_{ic}$  remains constant in the rarefaction interval,  $\omega$  might also remain unchanged. In this case, we can confidently predict that  $\nu_{bf}^{obs}$  should decrease in the rarefaction interval. On the other hand, the ion inertial scale theory for dissipation also embraces non-wave processes such as current sheet formation [Leamon *et al.*, 2000]. For these processes, it is less clear what value is appropriate to use for  $\omega$ . As a result, it is difficult to predict what will happen within the rarefaction interval to the  $\omega$  term in  $\nu^{obs}$  in the case of the ion inertial scale predictions. It is possible that  $\omega$  will decrease and contribute further to the decrease in  $\nu_{bf}^{obs}$ . However,  $\omega$  might increase. In order to cancel out the significant decrease associated with  $\mathbf{k} \cdot \mathbf{V}_{SW}$ , the value of  $\omega$  would have to undergo a very large increase in the rarefaction interval. Although we cannot rule out this possibility, it seems more likely that inertial-scale processes will lead to a decrease in  $\nu_{bf}^{obs}$ .

Thus, there is a clear contrast in the predictions of what should happen to  $\nu_{bf}$  in the rarefaction interval. The data show a clear decrease in  $\nu_{bf}^{obs}$ . This suggests that the

onset of dissipation is associated with processes which occur at the ion inertial length because only this length scale predicts a decrease of  $\nu_{\text{bf}}$ .

The question of the orientation of  $\mathbf{k}$  relative to  $\mathbf{V}_{\text{SW}}$  (as often factored through the orientation of the mean magnetic field) cannot be taken lightly. Changes in the relative orientation can be effected by either a bulk rotation of the mean field or by changes in the orientation of the wave vector relative to the mean field (which is commonly referred to as changes in the geometry). Our three-day interval can be divided into three regions according to the large-scale IMF direction. The first, preceding 18:00 UT on DOY 130, is characterized by large-amplitude, low-frequency fluctuations that average about a mean field that is close to what is seen throughout the next day. The second interval, extending to the end of DOY 131, has a very constant field direction. Both intervals show a mean field that is in good agreement with the *Parker* [1961, 1963] prediction. Interval 3, on DOY 132, displays a greater degree of large scale IMF fluctuations, an extended period when the mean field direction is perpendicular to the flow, and a field reversal late in the day. The azimuthal mean field may bring nearly perpendicular wave-vectors [*Matthaeus et al.*, 1990; *Bieber et al.*, 1996; *Leamon et al.*, 1998a] more nearly into alignment with the flow and explain the increased spectral break frequency relative to that of DOY 130. But the generally Parker-like field orientation on the first and second day means that the shift of the spectral break frequency to lower values on DOY 131 cannot be due to a change in the wave vector geometry.

Integration of the geometry, or percent slab, analysis into the dissipation discussion yields results consistent with *Leamon et al.* [1998a]. The slab fraction is larger in the

dissipation range than in the inertial range in all but one period we have analyzed. This suggests that dissipation of the 2-D component is the leading means for forming the dissipation range and this is consistent with ion inertial scale processes [Leamon *et al.*, 1999; 2000].

### 3. Summary

We have taken advantage of an exceptional parcel of solar wind to address issues of macrophysics and microphysics in the solar wind. Key features of this parcel (which was observed by ACE on May 10-12, 1999) are its very low density, its low temperature, constant magnetic field strength, and high Alfvén speed  $V_A$ . The ACE spacecraft remained inside this rarefaction interval for  $\sim$ forty-eight hours.

Turning first to issues of macrophysics, we note that inside the rarefaction interval the RMS magnetic fluctuation levels,  $B_{\text{RMS}}$ , are significantly reduced relative to the levels outside the parcel. Moreover, the waves inside the parcel are more Alfvénic (i.e., less compressive) than those outside. This is reminiscent of some Ulysses observations at low latitudes and varying heliocentric distances reported by Buttighofer *et al.* [1999] who identified similar solar wind “channels” as regions of nearly scatter-free propagation for energetic solar electrons. Buttighofer *et al.* found that inside the channels, ion densities are low and the  $B_{\text{RMS}}$  fluctuation levels are strikingly reduced (by a factor of 10) relative to ambient levels. The magnetic fluctuations inside the channels are also found to be more Alfvénic than those outside. The channels were observed to last several hours. We consider that these channels, with their large  $V_A$  values, exhibit striking similarities

to the rarefaction interval of May 10–12, 1999. However, in the absence of published plasma temperatures, the values of the plasma  $\beta$  parameter in the Buttighofer channels are unknown.

In the context of the *Uchida* [1973] model, we expect that fast-mode waves in the solar wind cannot enter the May 11, 1999 parcel (or the Buttighofer et al. channels) because of refraction. Thus, the level of fast-mode waves in the parcel must be lower than that outside. This leads to an accompanying reduction in the compressive components inside the parcel, as observed.

In any discussion of refraction, we recognize that there is a minimum size for ray optics to be applicable. We have examined  $2\frac{1}{2}$  years of ACE solar wind data with this in mind. When we examine increasingly large parcels that can be uniformly characterized by a single value of  $V_A$ , the presence of large  $V_A$  appears to correlate with a reduction in the fluctuation level. This effect sets in with a minimum flux tube size of  $\sim 16$  min. Our results are consistent with the expectation that refraction effects make their appearance provided that the flux tubes are of a certain minimum linear extent. We note also that the *Buttighofer et al.* [1999] events were all 15 min to several hours in duration.

The implied refractive separation of wave modes may be somewhat mitigated when the apparent size and history of the rarefaction interval is considered. It is possible that the apparent refraction occurs continuously at all distances between the Sun and 1 AU, but that the growing spatial scale of the rarefaction interval and changing Alfvén speed limits the range of heliocentric distances where refraction is most effective. For instance, closer to the Sun,  $V_A$  would have been larger than we see at 1 AU if the plasma were

uniformly expanding, or  $V_A$  would be smaller if the solar wind expanded nonuniformly with a rarefaction interval of increasing radial extent [Usmanov *et al.*, 2000]. Such considerations are beyond the scope of this work, but may make refraction more or less efficient at different stages of the interval's expansion. Wherever the refraction occurs, once the rarefaction interval is depleted of fast-mode wave energy, and in the absence of large wind shears to drive local turbulence, it is likely that the region simply remains an area of overall depleted wave energy. The nature of refraction is such that whatever level of wave energy remained inside, it should be more Alfvénic (i.e. less compressive) than outside.

Turning now to microphysics, we have tested two theories for the dissipation of magnetic fluctuations in the solar wind. Our test takes advantage of the unusually low  $\beta$  value on May 11, 1999. We find that dissipation in the solar wind is controlled by physical processes that occur at the ion inertial length scale. Our data are not consistent with dissipation due to ion cyclotron resonance. In principle, the Ulysses channels reported by *Buttighofer et al.* [1999] might also have been low- $\beta$  sites and suitable to exploit the gap which opens up between  $k_{ii}$  and  $k_{ic}$  in regions of low  $\beta$ . However, *Buttighofer et al.* did not report values of  $\beta$ , so we cannot predict how wide the gap might have been.

**Acknowledgments.** Efforts at the Bartol Research Institute were supported by CIT subcontract PC251439 under NASA grant NAG5-6912 for support of the ACE magnetic field experiment and by the NASA Delaware Space College Grant. Work at Los Alamos was

performed under the auspices of the U.S. Department of Energy with financial support from the NASA ACE program.

## References

- Behannon, K. W., Observations of the Interplanetary Magnetic Field Between 0.46 and 1 AU by the Mariner 10 Spacecraft, Ph.D. thesis, Catholic Univ. of Am., Washington, DC, 1975.
- Belcher, J. W., and L. Davis Jr., Large-amplitude Alfvén waves in the interplanetary medium, 2, *J. Geophys. Res.*, 76, 3534–3563, 1971.
- Bieber, J. W., W. Wanner, and W. H. Matthaeus, Dominant two-dimensional solar wind turbulence with implications for cosmic ray transport, *J. Geophys. Res.*, 101, 2511–2522, 1996.
- Buttighofer, A., Solar electron beams associated with radio Type III bursts: Propagation channels observed by Ulysses between 1 and 4 AU, *Astron. Ap.*, 335, 295–302, 1998.
- Buttighofer, A., L. J. Lanzerotti, D. J. Thomson, C. G. MacLennan, and R. J. Forsyth, Spectral analysis of the magnetic field inside particle propagation channels detected by Ulysses, *Astron. Ap.*, 351, 385–392, 1999.
- Coleman, P. J., Jr., Turbulence, viscosity, and dissipation in the solar wind plasma, *Astrophys. J.*, 153, 371–388, 1968.
- Crooker, N. U., S. Shodham, J. T. Gosling, J. Simmerer, R. P. Lepping, J. T. Steinberg, and S. W. Kahler, Density extremes in the solar wind, *Geophys. Res. Lett.*, 27, 3769–3772, 2000.
- Leamon, R. J., C. W. Smith, N. F. Ness, W. H. Matthaeus and H. K. Wong, Observational constraints on the dynamics of the interplanetary magnetic field dissipation range, *J. Geophys. Res.*, 103, 4775–4787, 1998a.
- Leamon, R. J., W. H. Matthaeus, C. W. Smith, and H. K. Wong, Contribution of cyclotron-

- resonant damping to kinetic dissipation of interplanetary turbulence, *Astrophys. J. Lett.*, *507*, L181-L184, 1998b.
- Leamon, R. J., C. W. Smith, N. F. Ness and H. K. Wong, Dissipation range dynamics: Kinetic Alfvén waves and the importance of  $\beta_e$ , *J. Geophys. Res.*, *104*, 22,331–22,344, 1999.
- Leamon, R. J., W. H. Matthaeus, C. W. Smith, G. P. Zank, D. J. Mullan and S. Oughton, MHD driven kinetic dissipation in the solar wind and corona, *Astrophys. J.*, *537*, 1054–1062, 2000.
- Matthaeus, W. H., M. L. Goldstein, and D. A. Roberts, Evidence for the presence of quasi-two-dimensional nearly incompressible fluctuations in the solar wind, *J. Geophys. Res.*, *95*, 20,673–20,683, 1990.
- Matthaeus, W. H., G. P. Zank, C. W. Smith and S. Oughton, Turbulence, Spatial Transport, and Heating of the Solar Wind, *Phys. Rev. Lett.*, *82* (17), 3444–3447, 1999.
- McComas, D. J., S. J. Bame, P. Barker, W. C. Feldman, J. L. Phillips, P. Riley, and J. W. Griffée, Solar wind electron proton alpha monitor (SWEPAM) for the Advanced Composition Explorer, *Space Sci. Rev.*, *86* (1-4), 563–612, 1999.
- Parker, E. N., The interplanetary gas and magnetic field, in *Science in Space*, edited by L. V. Berkner and H. Odishaw, McGraw Hill, New York, 1961.
- Parker, E. N., *Interplanetary Dynamical Processes*, Wiley-Interscience, New York, 1963.
- Richardson, I. G., D. Berdichevsky, M. D. Desch, and C. J. Farrugia, Solar-cycle variation of low density solar wind during more than three solar cycles, *Geophys. Res. Lett.*, *27*, 3761–3764, 2000.
- Schwartz, S. J., W. C. Feldman, and S. P. Gary, The source of proton anisotropy in the high-speed solar wind, *J. Geophys. Res.*, *86*, 541–546, 1981.

- Smith, C. W., M. H. Acuña, L. F. Burlaga, J. L'Heureux, N. F. Ness, and J. Scheifele, The ACE magnetic field experiment, *Space Sci. Rev.*, *86* (1-4), 613–632, 1999.
- Smith, C. W., W. H. Matthaeus, G. P. Zank, N. F. Ness, S. Oughton, and J. D. Richardson, Heating of the low-latitude solar wind by dissipation of turbulent magnetic fluctuations,” *J. Geophys. Res.*, in press, 2000.
- Stix, T. H., *Waves in Plasmas*, Am. Inst. of Phys., College Park, Md., 1992.
- Thompson, B. J., J. B. Gurman, W. M. Neupert, J. S. Newmark, J.-P. Delaboudinire, O. C. St. Cyr, S. Stezelberger, K. P. Dere, R. A. Howard, and D. J. Michels, SOHO/EIT Observations of the 1997 April 7 Coronal Transient: Possible Evidence of Coronal Moreton Waves”, *Astrophys. J.* *517*, L151, 1999.
- Uchida, Y., Flare-induced MHD disturbances in the corona: Moreton waves and Type II shocks”, in *High Energy Phenomena in the Sun*, edited by R. Ramaty and R. G. Stone, NASA SP-342, p. 577–588, 1973.
- Usmanov, A. V., M. L. Goldstein, and W. M. Farrell, A view of the inner heliosphere during the May 10-11, 1999 low density anomaly, *Geophys. Res. Lett.*, *23*, 3765–3768, 2000.
- Zank, G. P., W. H. Matthaeus, and C. W. Smith, Evolution of turbulent magnetic fluctuation power with heliospheric distance, *J. Geophys. Res.*, *101*, 17,093–17,107, 1996.

---

D.J. Mullan, N.F. Ness, and C.W. Smith, Bartol Research Institute, University of Delaware, Newark, DE 19716. (e-mail: {mullan; nfness; and chuck}@bartol.udel.edu)

R.M. Skoug and J. Steinberg, Los Alamos National Laboratory, Los Alamos, NM 87545. (e-mail: {rskoug; and jsteinberg}@lanl.gov)

Received \_\_\_\_\_

Submitted to *Journal of Geophysical Research* (Space Physics): January 19, 2001.

Revised and Resubmitted: March 5, 2001.

**Figure 1.** Days 130 through 132 of 1999 when the solar wind density is observed to drop to  $0.1 \text{ p cm}^{-3}$ . IMF intensity  $B$  [nT], IMF longitude  $\delta$  [degrees], and IMF latitude  $\lambda$  [degrees], as well as RMS level of the IMF fluctuations  $B_{\text{RMS}}$  [nT] are provided by the MAG instrument. The radial component of the wind speed  $V_R$  [ $\text{km s}^{-1}$ ], proton density  $N_P$  [ $\text{cm}^{-3}$ ] and proton temperature  $T_P$  [K] are provided by the SWEPAM instrument. The proton  $\beta$  and Alfvén speed  $V_A$  [ $\text{km s}^{-1}$ ] are computed from data supplied by both instruments. The anisotropy of the IMF fluctuation spectra  $E_{\perp}^B/E_{\parallel}^B$  in the inertial range and dissipation ranges are shown along with the anisotropy of the wave vector (expressed in terms of percent slab component in the inertial and dissipation ranges).

**Figure 2.** The unusually low RMS level [nT] of the IMF fluctuations during the interval in question is demonstrated by computing the distribution of RMS levels (top) over the period DOY 1, 1998 through DOY 169, 2000. The integral over the distribution from 0 to the prescribed value (bottom) emphasizes this point.

**Figure 3.** Average RMS levels [nT] as a function of Alfvén speed [ $\text{km s}^{-1}$ ] for intervals of finite duration and like-valued RMS. Vertical uncertainties are determined by the variance of the distributions and horizontal uncertainties denote the bin width for  $V_A$ .

**Figure 4.** Power spectral density for 5 intervals of IMF measurements with the trace of the PSD matrix, the PSD of the component parallel to the mean field, and the PSD of  $|\mathbf{B}|$  shown. The intervals are (a) 130/0:00–12:00 UT, (b) 130/12:00–18:00 UT, (c) 131/6:00–24:00 UT, (d) 132/0:00–12:0 UT, and (e) 132/6:00–24:00 UT. Note the decreased level of the  $|\mathbf{B}|$  and parallel component PSD during the time of reduced  $N_P$ .

**Figure 5.** Frequency subset of the trace curves shown in Figure 4 labelled (a)–(e) as before. The frequency at which each measured spectra breaks from the inertial range to the dissipation range is marked with an arrow. Note the decreasing spacecraft frequency associated with this break feature as the solar wind density is reduced.

**Table 1.** Spectral Break Frequencies

	DOY/Hrs [UT]	$\nu_{bf}^{obs}$ [Hz]
(a)	130/0:00-12:00	$0.230 \pm 0.002$
(b)	130/12:00-18:00	$0.176 \pm 0.009$
(c)	131/6:00-24:00	$0.168 \pm 0.004$
(d)	132/0:00-12:00	$0.260 \pm 0.002$
(e)	132/6:00-24:00	$0.437 \pm 0.006$

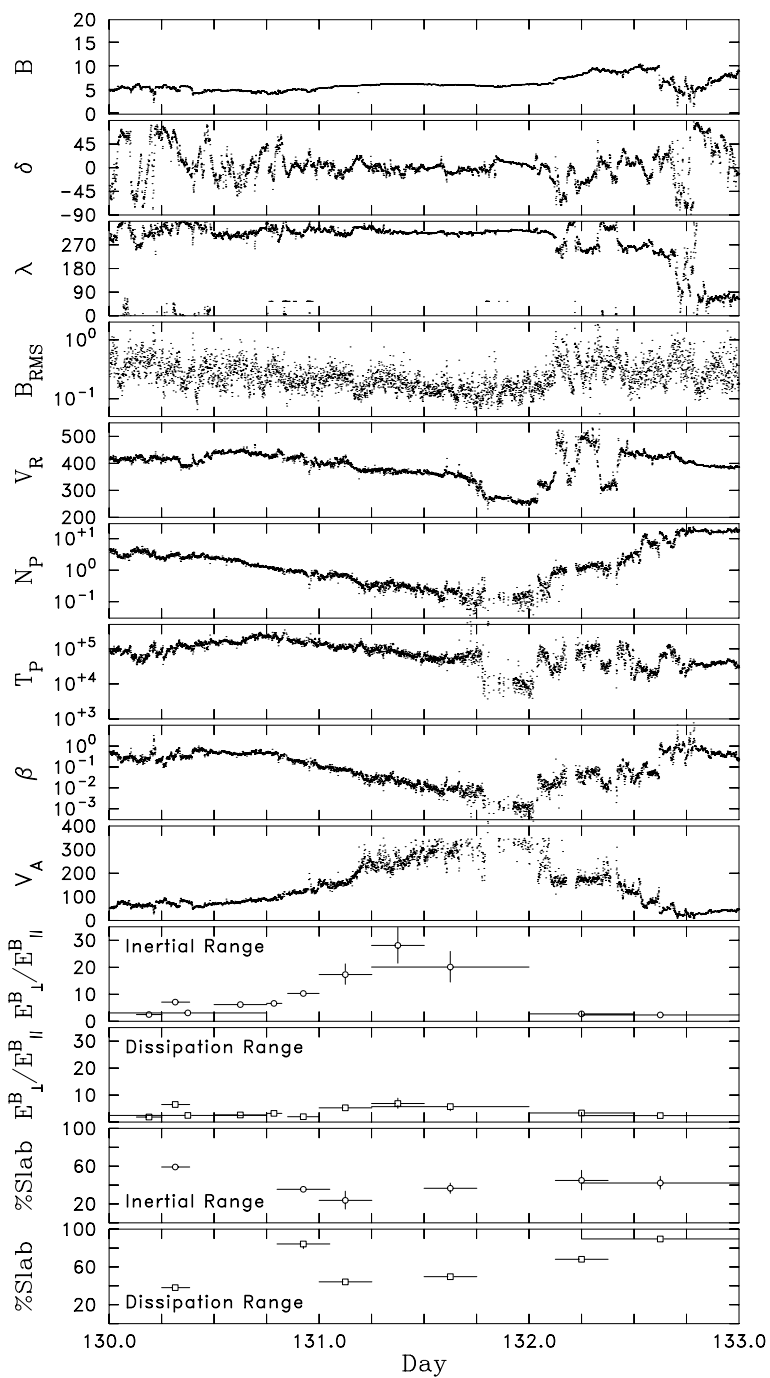


Figure 1.

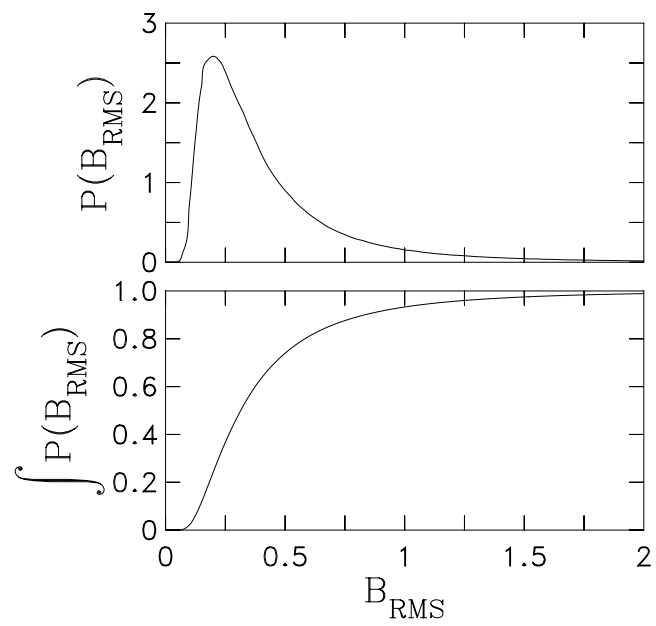


Figure 2.

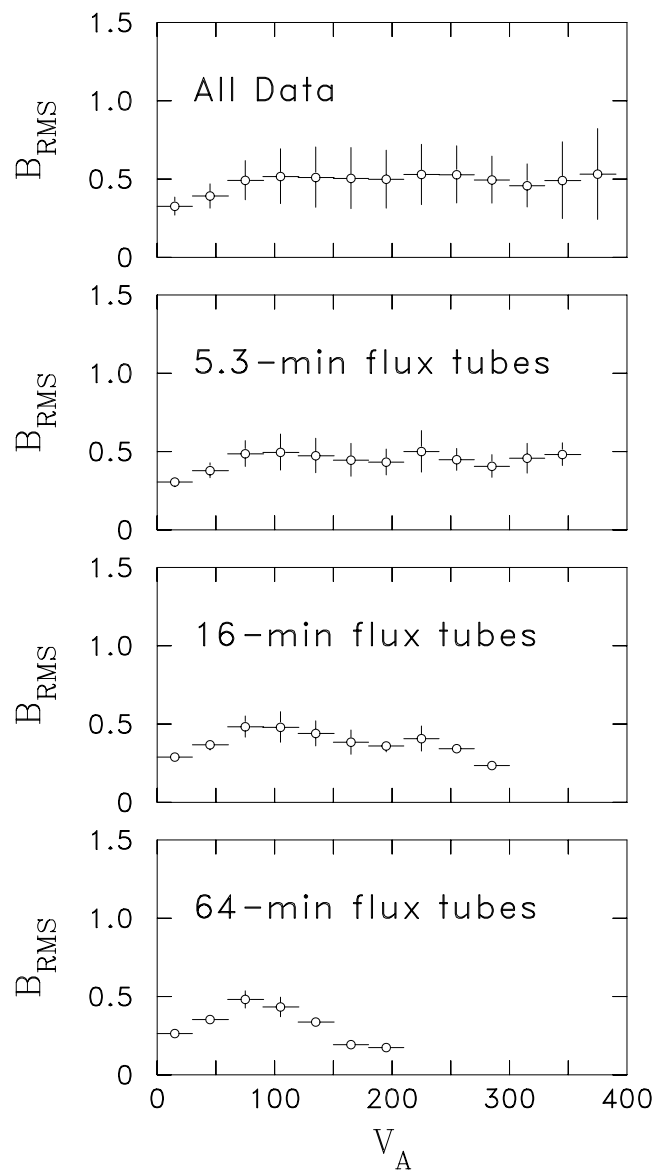


Figure 3.

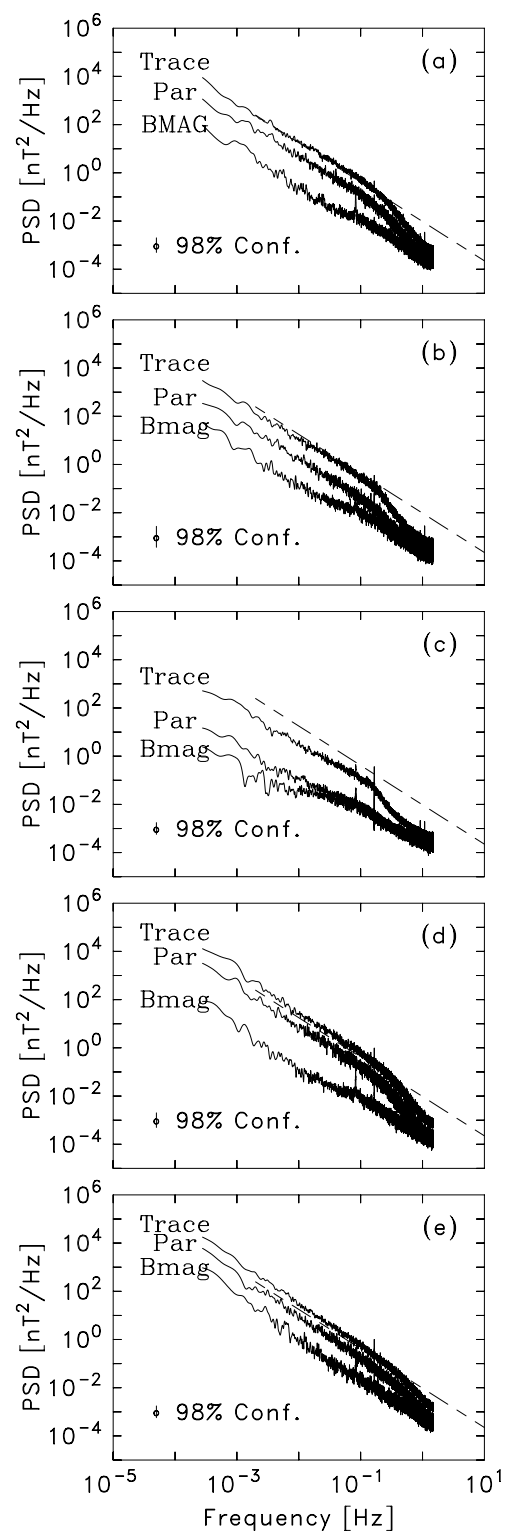


Figure 4.

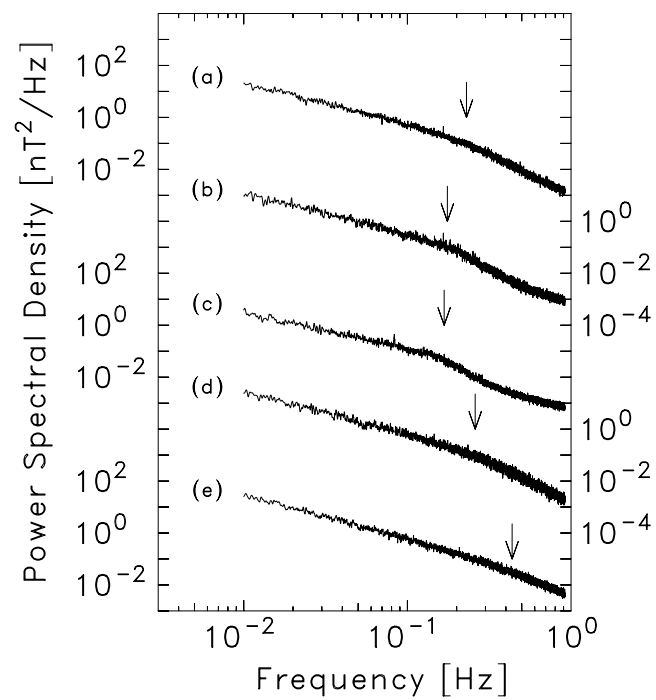


Figure 5.